

## Study the Influence of Antimony Dopant and Annealing on Structural, Optical and Hall Parameters of AgInSe<sub>2</sub> Thin Film

**Suha Nabeel Sobhi**

Department of Physics, College of  
Education for Pure Sciences-Ibn-Al-Haitham, University  
of Baghdad, Baghdad, Iraq.  
[soha.nabeel1204a@ihcoedu.uobaghdad.edu.iq](mailto:soha.nabeel1204a@ihcoedu.uobaghdad.edu.iq)

**Bushra H. Hussein**

Department of Physics, College of  
Education for Pure Sciences-Ibn-Al-Haitham,  
University of Baghdad, Baghdad, Iraq.  
[boshra.h.h@ihcoedu.uobaghdad.edu.iq](mailto:boshra.h.h@ihcoedu.uobaghdad.edu.iq)

**Article history: Received, 6, March, 2022, Accepted, 3, April, 2022, Published in July 2022.**

**Doi:10.30526/35.3.2824**

### Abstract

Sb-doped AgInSe<sub>2</sub> (AIS: 3%Sb) thin films were synthesized by thermal evaporation with a vacuum of  $7 \times 10^{-6}$  torr on glass with (400+20) nm thickness. X-ray diffraction was used to show that Sb atoms were successfully incorporated into the AgInSe<sub>2</sub> lattice. Then the thin films are annealed in air at 573 K. XRD shows that thin films AIS pure, AIS: 3%Sb and annealing at 573 K are polycrystalline with tetragonal structure with preferential orientation (112). raise the crystallinity degree. The Absorption spectra revealed that the average Absorption was more than 60% at the wavelength range of 400–700 nm. UV/Visible measure shows the lowering in energy gap to 1.4 eV for AIS: 3%Sb at 573 K. This energy gap making these samples suitable for photovoltaic application, The electric property was better when AgInSe<sub>2</sub>: 3%Sb at 573 K, thin films were of donor type and the concentration of electrons in them increased with increasing Sb doped and annealing temperature.

**Keywords:** AgInSe<sub>2</sub>, Antimony, AIS: 3%Sb thin films, XRD, Optical parameters.

### 1. Introduction

The chalcopyrite thin films like AgInSe<sub>2</sub> which have tetragonal crystallizes and is a crystal structure for  $A_{II}B_{III}C_{2VI}$  where (A= Ag, Cu, B= Ga, Al, In and C= Se, S, Te). These compounds are analogs to binary zinc blend II-VI. Silver-based chalcopyrite semiconductor has as better candidates for solar cell fabrication [1]. Ternary Silver Indium Diselenide (AIS) is a typical n-type semiconductor [2,3] that possesses direct gap energy [4] lies between 0.8 and 2.0 eV [5] high optical absorption ( $\sim 10^5 \text{ cm}^{-1}$ ), (AgInSe<sub>2</sub>) is the best-promised absorber materials for photovoltaic cell [6]. In many works doping AIS with different elements such as boron (B) doping on AgInSe<sub>2</sub> by ion implantation and heat-treatment technique desired behaviors for photoconductive of the B- AgInSe<sub>2</sub> thin film when 473K [7]. The influence of germanium (Ge) doping on the AgInSe<sub>2</sub> thin film properties has been studied with good optical transmittance spectra and the conductivity from type [2]. The electrical conductivity enhancements about



three orders by doping Tin (Sn) in the Ag sites in n-type, the increased conductivity for the films shows the Sn in AgInSe<sub>2</sub> film as better applicants for fabrication of p–n junction in PV [8]. Found that the effects of Zinc (Zn) doping in AgInSe<sub>2</sub> the Fermi level tend to shift toward the conduction band when Zn is a substitute for the Ag and forms the active donor defects, increasing the carrier concentration ND and decreasing the lattice thermal conductivity by modifying the crystal structure [9].

Several techniques used to fabrication AIS, such as spray pyrolysis technique [10,11], reactive evaporation [8], pulsed electrodeposition technique [12]. co-evaporation [13], sol–gel spin-coating technique [14]. hybrid sputtering/evaporation process [15]. DC magnetron sputtering [16], chemical bath deposition [17]. hot-press method [18]. thermal evaporation with different ion uences [19]. thermal evaporation with annealing [20]. electrodeposition process [21]. Bridgman technique [22]. Simple Chemical Method [23]. the crystal structure of AIS is tetragonal structure chalcopyrite with the lattice constant a = b = 6.102 Å and c = 11.69 Å [11]. AgInSe<sub>2</sub> blended organic–inorganic solar cells were fabricated and obtained was efficiency of 0.2% [24] Doping of Antimony (Sb) in AIS occupies the cation (Ag or In) site, rather than the anion (Se) site since the relative electronegativity of Sb (2.05) compared to those of Ag (1.93) or In (1.78) or Se (2.55), the ionic radii is a major factor uses for choosing applicable contribution materials [23]. Structural, optical and electrical properties of AIS film could be controlled for example the ionic radius of Antimony is close to the ionic radius of Ag, In and Se ions. Sbis suitable dopant for AIS because the Sb ionic radii (0.9 Å) while Ag<sup>+1</sup> (1.29 Å), In<sup>+3</sup> (0.94 Å), Se<sup>-4</sup> (0.56 Å) [25,26].

This study aims to concentrate on the effect of (Sb) doped on the optical structural properties and all Effects of AgInSe<sub>2</sub> film and the interconnection between these parameters.

## 2. Experimental

From highly purity (99.99%) of Silver (Ag) Indium (In) and Diselenide (Se) elements with stoichiometric proportions (1:1:2) to prepare: 3%Sb thin films, these elements were put in a quartz tube with a vacuum ( $4.5 \times 10^{-4}$  mbar), these three elements heated up to (1100K) was higher than the melting temperature of AgInSe<sub>2</sub> (1050 K) [19]. In an electric furnace for six hours in the end the alloy is left to cool to room temperature. AIS: 3%Sb thin films (pure and doped at 573K) were deposited by the thermal evaporation method ( $6 \times 10^{-6}$  torr) on glass substrates with 400 nm thickness. 3%Sb doping methods were carried out by using the thermal diffusion at 473 K in an electric furnace for 60 minutes. X-ray diffraction has been used to study the structure of these films by detailed  $2\theta$  from  $20^\circ$  to  $80^\circ$  with intervals of  $0.05^\circ$ , Scherer's Formula was used to calculate the crystalline size of the films [27, 28]:

$$C.S = \frac{0.9\lambda}{B \cos\theta} \quad (1)$$

where 0.9 is the shape factor and B(FWHM). is the width of the diffraction peak at half maximum intensity.

The optical interferometer method was used to determine the thickness of AgInSe<sub>2</sub>: 3%Sb samples. Optical properties of thin film preparation, transmission and absorption spectrums in the range between (400 to 1000) nm have been noted, and Lambert law and Tauc equation have been used to determine the absorption coefficients  $\alpha$  and the energy gap ( $E_g^{opt}$ ) respectively from the absorption spectrum [27,29]:

$$\alpha h\nu = D (h\nu - E_g)^r \quad (2)$$

$$\alpha = 2.303 \frac{A}{t} \quad (3)$$

where D is a constant depending on the temperature and the properties of the valence & conduction bands and  $\alpha$ : the absorption coefficient,  $h\nu$  the incident photon energy,  $r$ : is a parameter for the type of the optical transition. A: absorbance, t: thickness.

Optical Constants such as k: extinction coefficient, n refractive index, real part  $\epsilon_r$  & imaginary part  $\epsilon_i$  of dielectric constant can be considered by the relations below: [30,31,32]:

$$k = \frac{\alpha\lambda}{4\pi} \quad (4)$$

$$n = \left[ \frac{4R}{(R-1)^2} - k^2 \right]^{1/2} - \frac{(R+1)}{(R-1)} \quad (5)$$

$$\epsilon_r = n^2 - k^2 \quad (6)$$

$$\epsilon_i = 2nk \quad (7)$$

The Hall Effect results showed the type of thin film of AgInSe<sub>2</sub>: 3%Sb has been calculated by the relations below [31]:

$$R_H = \left( \frac{V_H}{I_x} \right) \frac{t}{B_z} \quad (8)$$

$$p = \frac{1}{qR_H} \quad (p - \text{type}) \quad (9)$$

$$n = \frac{-1}{qR_H} \quad (n - \text{type}) \quad (10)$$

When The Hall coefficient ( $R_H$ ), electric current ( $I_x$ ) and Hall voltage ( $V_H$ ), magnetic field ( $B_z$ ).

### 3. Result and Discussion:

Figure (1) displays XRD for AIS pure and AgInSe<sub>2</sub>: 3%Sb doped at RT and 573 K when the thickness (400) nm deposition on glass substrates, All the samples show polycrystalline for films have tetragonal structural with main to distinguishable peak when  $2\theta \approx 25.726^\circ$  when the preferred orientation (112)[1,10] and another peak appear at  $2\theta$  equal to  $42.97^\circ$  when the orientation (204). Table (1) show our study, the comparison with the ICDD 00-038-0952 card standard value very good matched, the degree of crystalline increasing when AgInSe<sub>2</sub>: 3%Sb dopant and annealing at 573 K. Peak main intensity of (112) was increased with the addition of 3%Sb comparison with that for AgInSe<sub>2</sub> and shifts approximately  $3^\circ$  to lower  $2\theta$  angle in comparison with that for AgInSe<sub>2</sub> because that the Sb atomic "radius" (0.9 Å) smaller than that for In (0.94 Å) and Ag (1.29 Å). The increase of intensity refers to include of Sb atom in the progress to the growth of crystallinity. No diffraction peak related to Sb was observed from the XRD patterns. It was illustrated that Sb ion replaces or enters the interstitials of AIS as shown in the same Table. The FWHM decreases with Sb content added so subsequently the crystallite size is increased as calculated by equation (1). The effect of annealing at 573 K & 1h is similar to that of as-deposited thin films. However, annealed thin films show higher crystalline quality compared to as-deposited thin films this may be attributed to the nucleation formation.

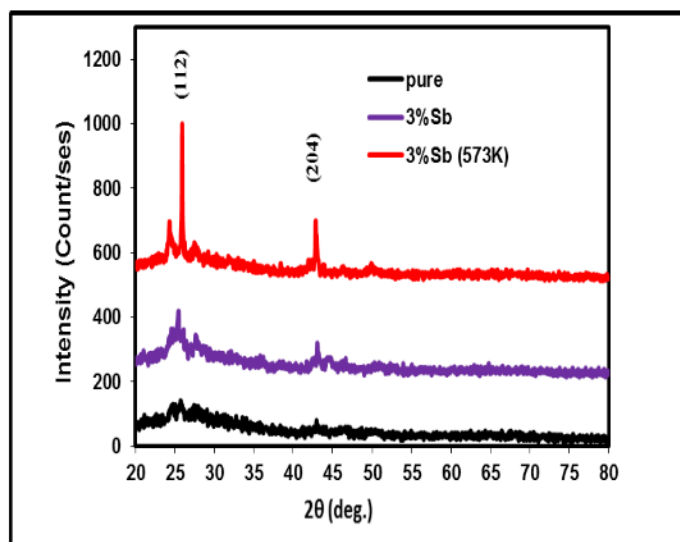


**Figure 1.** XRD Pattern for pure AIS film, AIS: 3%Sb doped and AgInSe<sub>2</sub>: 3%Sb doped after annealing to T=573 K.

**Table 1.** Data of XRD for pure AgInSe<sub>2</sub> film, 3% (Sb) and 3% (Sb) at T=573 K.

Thin Films	d(Std.) (Å)	d(Exp.) (Å)	2θ (Std.) (Deg.)	2θ (Exp.) (Deg.)	hkl	FWHM (deg.)	C.S (nm)
pure	3.46	3.4651	25.726	25.7	112	1.000	8.5149
	2.103	2.1012	42.97	42.95	204		
3% (Sb)	3.46	3.4918	25.726	25.5	112	0.317	26.8505
	2.103	2.0994	42.97	43.05	204		
3% (Sb) T=573 K	3.46	3.4373	25.726	25.9	112	0.231	36.8788
	2.103	2.1092	42.97	42.85	204		

**Figure (2)** and **Table (2)** show the optical properties and the effect of **3% (Sb)** and annealing 573K on transmittance and absorbance spectra of thin AIS films in the range 400-1000 nm. It is observed that the absorbance of all thin films increases with decreasing the wavelength. This may be due to decreasing the corresponding transmittance with decreasing the wavelength. The type and value of optical energy gap ( $E_g^{opt}$ ) for AIS, **3% (Sb)** and annealing at 573K thin films are determined using Taucs Equation (2), the allowed direct transitions occur in a thin film. This result agrees with R. Panda et. al.[19]. The absorption coefficients ( $\alpha$ ) which were of order  $10^4$  in these films were calculated from the absorbance spectra.

It is obvious from **Figure (3)** that the energy gap decreased to 1.4(eV) which has significant for optoelectronic device applications. This behavior may be attributed to the advance in the film's crystallite size. The calculated energy gaps are listed in Table (2). The value of the refractive index ( $n$ ), the extinction coefficient ( $k$ ) and the real and imaginary parts of the dielectric constant ( $\epsilon_r$ ,  $\epsilon_i$ ) for AIS thin film are calculated from equations (3-7). The calculated values of optical constant at the wavelength ( $\lambda$ ) equal to 500nm are listed in **Table (2)**. The refractive index  $n$  is a significant parameter for optical material and application. The values of  $n$  decrease with doping **3% (Sb)** and annealing temperature (in the visible region) due to a decrease in the corresponding reflection and attributed to an increase in the carrier concentrations in AIS thin film, this result agrees with Suresh Pall et. al.[32]. The extinction coefficient increases as seen in **Table (2)** takes the same behavior as the absorption coefficient because the extinction coefficient is directly related to the absorption of the light as in equation (4). The fundamental electron excitation spectrum of the film was termed using the frequency dependency of the complex dielectric constant. The real ( $\epsilon_r$ ) and imaginary ( $\epsilon_i$ ) parts of the dielectric constant are related to the  $n$  and  $k$  values and the value of  $\epsilon_r$  and  $\epsilon_i$  at  $\lambda=500$ nm

decreases because the behavior of  $\epsilon_r$  is similar to that of the  $n$  equation (6), while the behavior of  $\epsilon_i$  is similar to that of  $k$  because it mainly depends on the  $k$  value equation (7). The effect of doping 3% (Sb) and annealing on the value of  $\epsilon_i$  were smaller than that of the pure thin film, which indicates a small dielectric loss.

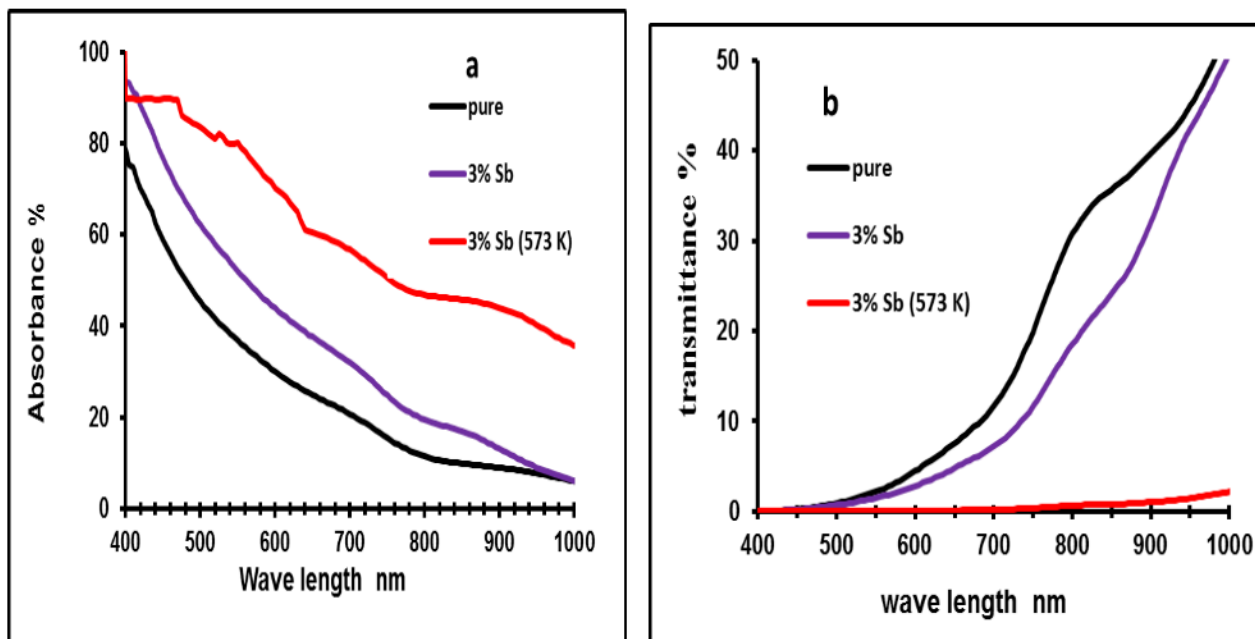


Figure 2. Transmittance and Absorption with wavelength for pure AgInSe<sub>2</sub> film, AIS: 3%Sb doped and AIS: 3%Sb doped after annealing to T=573 K.

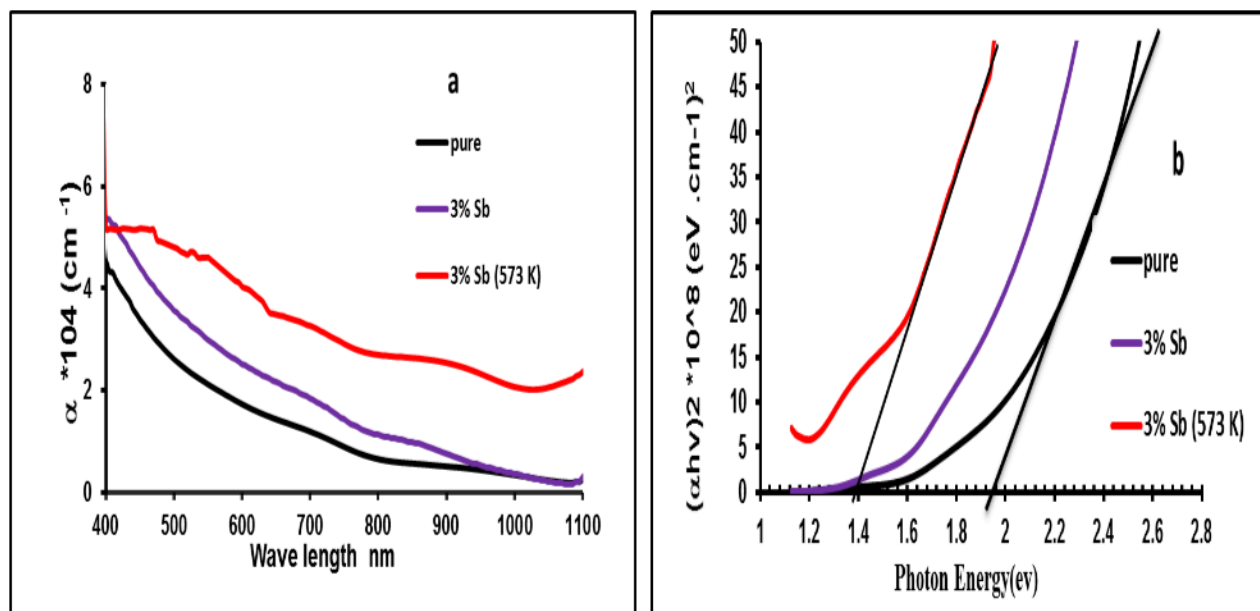
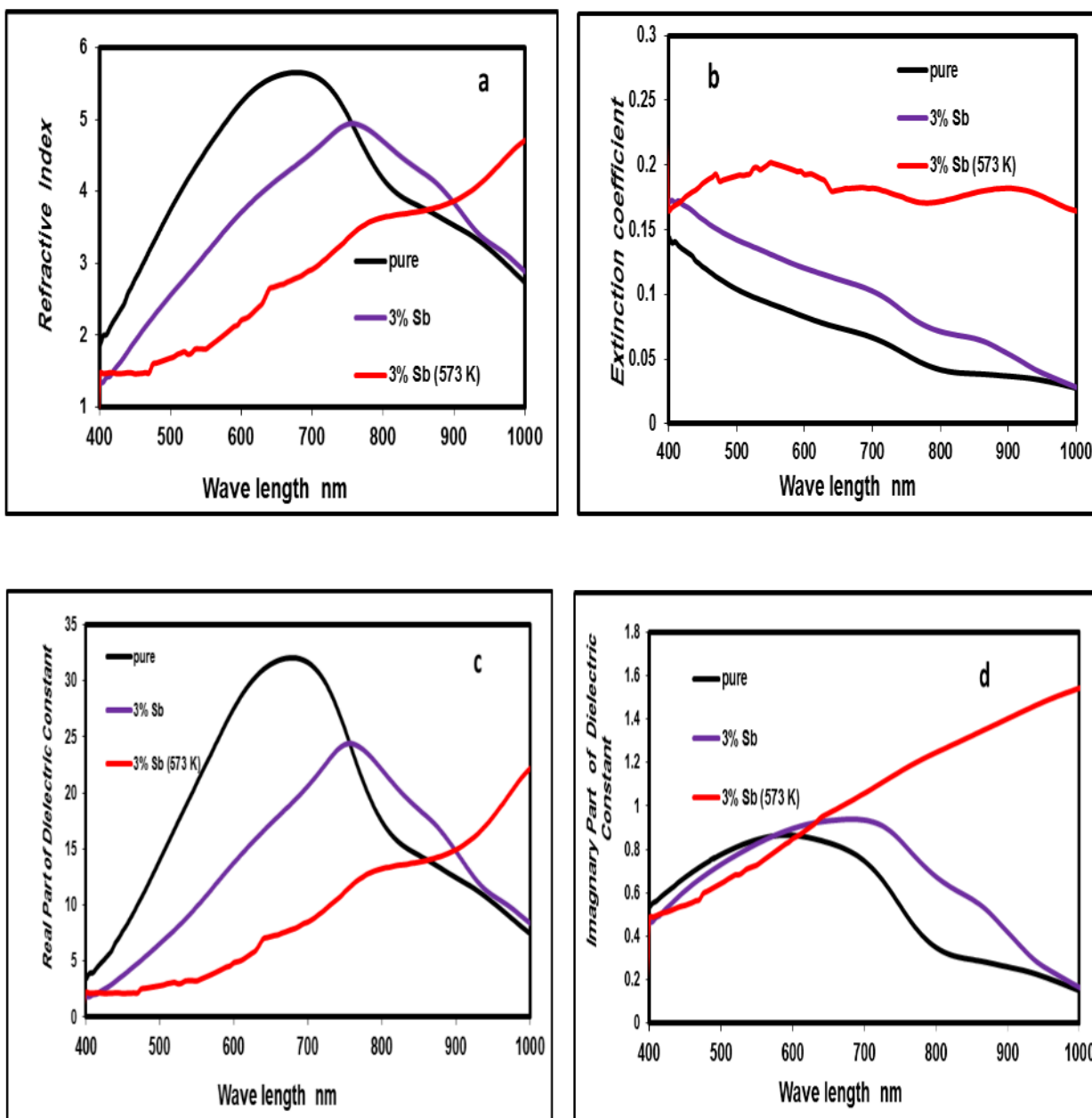


Figure 3. The  $\alpha$  vs. Wavelength and  $(\alpha h\nu)^2$  with  $h\nu$  plot of as prepared pure AgInSe<sub>2</sub> film, AIS: 3%Sb doped and AIS: 3%Sb doped after annealing to T=573 K.

**Table 2.** The optical parameters ( $E_g^{opt}$ ,  $\alpha$ ,  $k$ ,  $n$ ,  $\epsilon_r$  and  $\epsilon_i$ ) for pure AIS film, AgInSe2: 3%Sb doped and AgInSe2: 3%Sb doped after annealing to  $T=573$  K. where  $\lambda=500$ nm

Thickness (400nm)	$E_g^{opt}$ (eV)	$\alpha \times 10^4$ $cm^{-1}$	$n$	$k$	$\epsilon_r$	$\epsilon_i$
pure	1.96	2.61	3.7	0.103	14	0.77
3% (Sb)	1.75	3.58	2.55	0.14	6.52	0.72
3% (Sb) T=573 K	1.4	4.8	1.62	0.19	2.79	0.64



**Figure 4.** Variation of refractive index, Extinction coefficient, of the real and imaginary part of dielectric constant with wavelength for pure film, AgInSe2: 3%Sb doped and AgInSe2: 3%Sb doped after annealing to  $T=573$  K.

The type concentration of the charge carrier, resistivity and Hall mobility for pure, 3%Sb doped and AgInSe<sub>2</sub>: 3%Sb doped after annealing to T=573 K thin films have been estimated from Hall effect measurements, the calculated values are shown in **Table (3)**. From this Table, one can be noticed that the value of the Hall coefficient for all examined AgInSe<sub>2</sub> and 3%Sb doped thin films are negative which means that all the prepared samples exhibit n-type conductivity, i.e. the conduction is dominated by electrons. This is due to the donor centers formed during the deposition. This result agrees with previous investigations [2,3].

Moreover, it is seen that the carrier concentration increases with increasing annealing temperature due to an increase in the film grain size which leads to a decrease in the density of grain boundaries and thus reduces the electron trapping probability. As a result, the number of collisions between carriers will increase, which leads to a decrease in their mobility with increasing the annealing temperature.

**Table 3.**Electrical parameters from Hall effect measurements for AgInSe<sub>2</sub> thin films for pure AgInSe<sub>2</sub> film, AgInSe<sub>2</sub>: 3%Sb doped and AgInSe<sub>2</sub>: 3%Sb doped after annealing to T=573 K.

Thin Films	$R_H$ ( $\text{cm}^3/\text{C}$ )	$N_D$ ( $\text{cm}^{-3}$ )	$\mu_H$ ( $\text{cm}^2/\text{V.s}$ )	$\rho$ ( $\Omega.\text{cm}$ )
pure	-1973.47	$3.167 \times 10^{15}$	37.6342	52.43
3% (Sb)	-0.117261	$5.33 \times 10^{19}$	3.022983	0.03879
3% (Sb) T=573 K	-0.092183	$6.78 \times 10^{19}$	2.703724	0.034095

#### 4. Conclusions

Pure tetragonal AgInSe<sub>2</sub>: 3%Sb doped and AgInSe<sub>2</sub>: 3%Sb doped after annealing to T=573 K films were well synthesized by a thermal evaporation method. The grown AIS thin films were then doped with Sb at temperature 473 K by a thermal diffusion process. After doping, the crystallinity of the thin film was improved. Our findings show that the polycrystalline of tetragonal with (112) orientation crystal structure AgInSe<sub>2</sub> thin film from XRD. The grain size rose from XRD with 3%Sb doping. From the optical studies the 3%Sb doping into AgInSe<sub>2</sub> promoted a decreased band gap in comparison with the undoped AgInSe<sub>2</sub> chalcopyrite, the absorption coefficients increasing. The ability to improve the growth and quality of the grains structure, the Hall effect shows the conductivity type of the grown films remained n-type and the enhancement in the optical properties highlights 3%Sb doped AgInSe<sub>2</sub> to be applied as an absorber layer in films making these films suitable for photovoltaic application.

#### References

1. Bedi, R. K.; Pathak, D.; Deepak and D. Kaur, Structural and optical properties of AgInSe<sub>2</sub> films, *Z. Kristallogr. Suppl.*, **2008**, *27*, 177–183.
2. Yoshinori, E.; Hiroshi K.; and Takahiro T.; Ge Doping Effect on Properties of AgInSe<sub>2</sub> Thin Films, *Japanese Journal of Applied Physics*, **2002**, *44(3A)*, 1527-1531.
3. Yingcai Z.; Yong L.; Max W.; Nathan Z.; Koocher, Y. L.; Lijuan L.; Tiandou H.; James M.; Rondinelli, J.; Hong, G.; Jeffrey S.; and Wei X.; Synergistically Optimizing Carrier Concentration and Decreasing Sound Velocity in n-type AgInSe<sub>2</sub> Thermoelectrics, *Chemistry of Materials*, **2019**, *31*, 8182–8190.

4. Ahmad S.; and Mohib-ulHaq, M.; A study of energy gap, refractive index and electronic polarizability of ternary chalcopyrite semiconductors, *Iranian Journal of Physics Research*, **2014**, *14*, 89-93.
5. Qian, C.; Xihong, P.; and Candace K. Chan.,; Structural and Photoelectrochemical Evaluation of Nanotextured Sn-Doped AgInSe<sub>2</sub> Films Prepared by Spray Pyrolysis, *Chem Sus Chem*, **2013**, *6*, 102 – 109.
6. Arredondo1, C. A.; Mesa1, F.; and Gordillo1, G.; STUDY OF ELECTRICAL AND MORPHOLOGICAL PROPERTIES OF AgInSe<sub>2</sub> THIN FILMS GROWN BY CO-EVAPORATION, *IEEE*, **2010**, *978*, 002433–002438.
7. Olakoçlu, T. C.; Parlak, M.; Kulakci, M.; and Turan, R.; Effect of boron implantation on the electrical and photoelectrical properties of e-beam deposited Ag–In–Se thin films, *J. Phys. D: Appl. Phys.*, **2008**, *41*.
8. Rajani J.; Gunadhor S.; Okram, J. N.; Sudhanshu M.; and Rachel R. P.; Tin Incorporation in AgInSe<sub>2</sub> Thin Films: Influence on Conductivity, *The Journal of Physical Chemistry*, **2015**, *119*, 5727–5733.
9. Li W.; Pengzhan Y.; Yuan D.; Hong Z.; Zhengliang D.; and Jiaolin C.; Site occupations of Zn in AgInSe<sub>2</sub>-based chalcopyrites responsible for modified structures and significantly improved thermoelectric performance, *The Royal Society of Chemistry*, **2014**, *4*, 3897–33904.
10. Mahmood, F. A.; and Sayed, M. H.; Preparation and Characterization of Sprayed AgInSe<sub>2</sub> Thin Films, *Chalcogenide Letters*, **2011**, *8*, 10, 595 – 600.
11. Qian, C.; Xihong, Peng.; and Candace, K. Chan.; Structural and Photoelectrochemical Evaluation of Nanotextured Sn-Doped AgInSe<sub>2</sub> Films Prepared by Spray Pyrolysis, *ChemSusChem*, **2013**, *6*, 102 – 109.
12. Kulkarni, H. R.; Characterization and Optical Properties of AgInSe<sub>2</sub> Thin Films Prepared by Electrodeposition Technique, *International Research Journal of Management Science & Technology*, **2016**, *7*, 12, 190–197.
13. Arredondo, C. A.; Mesa, F.; and Gordillo, G.; STUDY OF ELECTRICAL AND MORPHOLOGICAL PROPERTIES OF AgInSe<sub>2</sub> THIN FILMS GROWN BY COEVAPORATION, *IEEE*, **2010**, *978*, 002433–002438.
14. Al-Agel F. A.; and Waleed E.; Mahmoud, Synthesis and characterization of highly stoichiometric AgInSe<sub>2</sub> thin films via sol–gel spin-coating technique, *Journal of Applied Crystallography*, **2012**, *45*, 921-925.
15. Little, S. A.; Ranjan, V.; Collins, R. W.; and Marsillac, S.; Growth analysis of (Ag,Cu)InSe<sub>2</sub> thin films via real time spectroscopic ellipsometry. *Appl. Phys. Lett.*, **2012**, *101*, 1-4.
16. Panda, R.; Naik, R.; Singh, U.P.; Mishra, N.C.; Thermal annealing induced modifications in structural, optical and microstructural properties of AgInSe<sub>2</sub> thin film, *International Conference on Materials Science & Technology, Oral / Poster*, **2016**.
17. Ching-Chen W.; Kong-Wei C.; Wen-Sheng C.; and Tai-Chou L.; Preparation and characterizations of visible light-responsive (Ag–In–Zn)S thin-film electrode by chemical bath deposition, *Journal of the Taiwan Institute of Chemical Engineers*, **2009**, *40*, 180-187.
18. Kenji Y.; Aya K.; Yasuhiro S.; Minoru O.; Keita Nomoto, T.; Yoshitake, S.; Ozaki, T.; Structural and electrical characterization of AgInSe<sub>2</sub> crystals grown by hot-press method, *Journal of Physics: Conference Series*, **2008**, *100*, 1-4.
19. Panda, R.; Khan, S. A.; Singh, U. P.; Naik R.; and Mishra, N. C.; The impact of fluence dependent 120 MeV Ag swift heavy ion irradiation on the changes in structural, electronic, and optical properties of AgInSe<sub>2</sub> nanocrystalline thin films for optoelectronic applications, *RSC Adv.*, **2021**, *11*, 26218–26227.
20. Iman H. K.; Fabrication of AgInSe<sub>2</sub> heterojunction solar cell, *AIP Conference Proceedings*, **2018**, *1968*, 030064–1-030064-7.



21. Mounir A.; Raquel D.; Fouzia C. E.; Arturo Tiburcio-Silver and Mohammed Abd-Lefdil, AgInSe<sub>2</sub> thin films prepared by electrodeposition process, *International Journal of Materials Science and Applications*, **2015**, 4, 35–38.
22. Hamdy T. S.; Melaad K. G.; Transport Properties of AgInSe<sub>2</sub> Crystals, *Materials Sciences and Applications*, **2014**, 5, 292-299.
23. Shehab, A. A.; Fadaam, S. A.; Abd, A. N.; Mustafa, M. H.; Antibacterial Activity Of ternary semiconductor compounds AgInSe<sub>2</sub> Nanoparticles Synthesized by Simple Chemical Method, *Journal of Physics: Conf. Series*, **2018**, 1003, 1-10.
24. Dinesh P.; Tomas W.; Tham A.; Nunzi, J.M.; Photovoltaic performance of AgInSe<sub>2</sub>-conjugated polymer hybrid system bulk heterojunction solar cells, *Synthetic Metals*, **2015**, 199, 87–92.
25. Shannon, R. D.; Revised effective ionic radii and systematic studies of interatomic distances in halides and chalcogenides. *Acta Crystallogr A.*, **1976**, 32 (5), 751–767.
26. Greenwood N. N.; and Earnshaw, v.; Chemistry of the Elements. *Elsevier*, **2012**.
27. Bushra K. H.; Characterization of n-CdO:Mg /p-Si Heterojunction Dependence on Annealing Temperature, *Ibn Al-Haitham Jour. for Pure & Appl. Sci.*, **2016**, 29, 3, 14–25.
28. Rana H. A.; Bushra H. H.; and Sameer A. M.; Effect of in on the properties of AlSb thin film solar cell, *AIP Conference Proceedings*, **2019**, 2123, 020030-1- 020030-9.
29. Bushra H.; Hanan, K. H.; Bushra. K. H.; Suad, H. A.; Effect of copper on physical properties of CdO thin films and n-CdO: Cu / p-Si heterojunction, *Journal of Ovonic Research*, **2022**, 18 (1), 37-41.
30. Sze S.; and Ng, K.; Physics of Semiconductor Devices, 3rd edition, *John Wiley and Sons*, **2007**.
31. Schroder, D.; Semiconductor Material and Device Characterization, *John Wiley & Sons*, **2006**.
32. Iman, H. K. and Bushra. H. H.; Study of Some Structural and Optical Properties of AgAlSe<sub>2</sub> Thin Films, *Ibn Al-Haitham Jour. for Pure & Appl. Sci.*, **2016**, 29 (2) ,41-51.